PHYSICAL REVIEW A **75**, 011402(R) (2007)

Strong optical forces from adiabatic rapid passage

X. Miao,[1] E. Wertz,[2] M. G. Cohen,[1] and H. Metcalf[1]
[1]*Physics Department, Stony Brook University, Stony Brook, New York 11794-3800, USA*
[2]*University of Paris VII, Paris, France*
(Received 13 September 2006; published 30 January 2007)

Periodic adiabatic rapid passage from counterpropagating light pulses is used in a parameter domain outside of the conventionally expected successful range to produce large optical forces on atoms by coherent control of the momentum exchange between the light and atoms. Both the magnitude and velocity range are much larger than those of the usual radiative force. We observed the force on metastable He atoms by the deflection of the atomic beam with periodic pulse sequences. We have also been able to map out the force magnitude in the two-dimensional parameter space of peak Rabi frequency and sweep range, and we find qualitative agreement with our model.

DOI: 10.1103/PhysRevA.75.011402 PACS number(s): 32.80.Pj, 42.50.Vk

We report the observation of very strong optical forces produced by coherent exchange of momentum between atoms and light fields implemented by adiabatic rapid passage (ARP). Such forces are caused by absorption from a light beam having $\vec{k}_1$ followed by stimulated emission into a beam of $\vec{k}_2 \neq \vec{k}_1$ where $|\vec{k}_j| = 2\pi/\lambda_j$. Guided by our calculations [1], we did these experiments in a domain of parameter space where the usual criteria for ARP are not very well satisfied.

For steady beams with $\vec{k}_2 = -\vec{k}_1$, the resulting standing wave produces an optical lattice, and its dipole force F_{dip} can be very much larger than the maximum value of the ordinary radiative force, $F_{rad} \equiv \hbar k \gamma/2$ ($1/\gamma \equiv \tau$ is the excited state lifetime). Other arrangements of the $\vec{k}$'s can produce comparably large forces. Although such dipole forces seem attractive as tools for manipulating atoms, their utility is limited because their sign alternates in space on the wavelength scale so their spatial average vanishes. Also, such controllable exchanges are reversible and therefore conservative, so they cannot be used for cooling: only the optical pumping among multiple atomic levels, enabled by spontaneous emission, can reduce the atomic phase space volume [2].

Recently we have been investigating the bichromatic force that arises from two beams of equal intensity and symmetrical detuning $\pm\delta$ from two-level atomic resonance ($|\delta| \gg \gamma$) [3–7]. (Each of the two counterpropagating beams has both frequencies.) This idea had been considered as far back as 1988 [8], observed in 1989 [9], and demonstrated again in 1997 [10]. The magnitude of this force is $\sim \hbar k \delta/\pi \gg F_{rad}$ and has a velocity capture range $v_c = \delta/k \gg \gamma/k$, where γ/k is the capture range of F_{rad}. Because of this huge v_c, Doppler compensation is unnecessary for slowing a thermal beam. Moreover, it has a strong velocity dependence at $\pm v_c$ as a result of irreversible nonadiabatic transitions [6] so that it can cool. The π-pulse model for describing this force provides an appealing intuitive description [8,10].

Motivated by this π-pulse picture that depends on the population inversion of a two-level system whose states are $|g\rangle$ and $|e\rangle$, we considered optical forces produced by ARP that also produce population inversions and are much more robust against variations of experimental parameters [11–13]. The laser parameters in our initial experiments were far from the requirements for ARP, but the results suggested further investigation [5,14].

From the Schrödinger equation, the evolution of the Bloch vector $\vec{R}$ on the Bloch sphere is determined by $\dot{\vec{R}} = \vec{\Omega}' \times \vec{R}$ [15,16]. We performed numerical studies of ARP in light that is both frequency and amplitude modulated in the form of multiply repeated chirped light pulses [1]. We found unanticipated confinement of orbits of $\vec{R}$ when the system was driven by a periodically varying torque vector $\vec{\Omega}'(t+2T_s) = \vec{\Omega}'(t) \equiv [\Omega(t), 0, \delta(t)]$ where $|\vec{\Omega}'| = \sqrt{\Omega^2 + \delta^2}$, the Rabi frequency $\Omega(t) \equiv [\langle e | e\vec{\mathcal{E}}(t) \cdot \vec{r} | g \rangle]/\hbar$, and the sweep time $T_s \equiv \pi/\omega_s$. This behavior led to a description similar to the Bloch theorem, but in time instead of the spatial domain. These nearly closed orbits were present even in ranges of Ω and δ where ARP is not expected to work well. Figure 1 shows a schematic of the timing scheme, modified by the inclusion of $2T_s$ gaps between pulse pairs for experimental reasons discussed below.

The chirped light pulses of ARP drive the atom-laser system up a ladder of dressed state energy sheets on sequential trajectories, thereby decreasing the atomic kinetic energy.

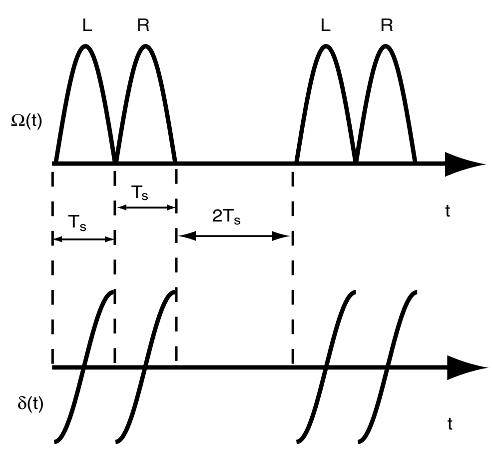

FIG. 1. The timing scheme illustrated. L and R stand for pulses coming from the right and left. The gap of $2T_s$ is to partly compensate for the effects of spontaneous emission (see below). The sequence repeats after $4T_s = 4\pi/\omega_s = 12.5$ ns.

One such step is shown by the heavy arrow on the dressed state energy surface of Fig. 1 of Ref. [1]. Nonadiabatic transitions between the energy surfaces must be avoided for this process to be effective.

To avoid such transitions in the usual scheme of ARP experiments where δ is swept but Ω is constant, there are certain requirements on the experimental parameters. First, the angle $\theta \equiv \tan^{-1}(\Omega/\delta)$ between $\vec{\Omega}'$ and the polar axis of the Bloch sphere must change slowly enough so that $\dot{\theta} \ll \vec{\Omega}'$ or $\dot{\delta} \ll \vec{\Omega}'^3/\Omega$. This means that $\vec{R}$ makes very many precessions about $\vec{\Omega}'$ during the sweep time T_s. (The usual scheme of ARP experiments is characterized by constant $\dot{\delta}$ so that $|\dot{\delta}| = 2\delta_0\omega_s/\pi$, where $\pm\delta_0$ is the sweep range.) This "adiabatic following" of $\vec{\Omega}'$ by $\vec{R}$ produces the "A" in ARP.

Second, $T_s \ll \tau$ to minimize the effects of spontaneous emission during the sweep, and thereby preserve coherence between the atom and the radiation field. In the usual scheme of ARP where $\dot{\delta}$ is constant, this becomes $\omega_s \gg \gamma$, or $|\dot{\delta}| \gg \delta_0\gamma$, and constitutes the "rapid" part of the name ARP. These two conditions on the sweep time T_s and the generalized Rabi frequency Ω' must be met independently, in addition to their combination $\Omega' \gg \gamma$.

Avoidance of nonadiabatic transitions is much more effective if $\delta_0 \gg \Omega(t=0)$ and $\Omega(t=\pi/\omega_s)$ so that $\vec{\Omega}'$ is very nearly polar at the extremes of the sweep. In our experiment, this is accomplished by synchronously varying the Rabi frequency with the optical frequency sweep, and thus it is quite different from the usual scheme of ARP. We have $\Omega(t) = \Omega_0|\sin \omega_s t|$ and $\delta = \pm \delta_0 \cos \omega_s t$, where the $\pm$ determines the sweep direction. We can vary Ω_0 and δ_0 independently, but they are generally of the same magnitude. The special case when they are equal has been solved analytically [17]. All these conditions can be written together as

$$\delta_0 \sim \Omega_0 \gg \omega_s \gg \gamma. \tag{1}$$

Sequential ARP passages are a very robust method for coherent exchange of momentum between atoms and the light field because they are not very sensitive to variations of the interaction time, the laser frequency, or the light intensity [1,18]. Moderate changes in the start and end point of the sweeps, corresponding to the Doppler shifts of a moving atom, are easily tolerated with little consequence as long as Eq. (1) is satisfied.

In our experiment, the chirped light pulses cross the atomic beam at 90° so they impart a transverse momentum impulse $\hbar k$ to the atoms. A simple model calculation of the magnitude of this force begins by considering the $\hbar k$ transferred in this first sweep of duration $T_s = \pi/\omega_s$ (=3.125 ns in our experiment, much shorter than the few μs passage time of the atoms through the light beam) leaving the atoms in the excited state. The pulse travels $\approx$47 cm to a retroreflecting mirror and then returns after the desired relative delay of $\pi/\omega_s = 3.125$ ns to drive the atoms back to the ground state and also transfer $\hbar k$. The next pulse pair arrives after $2T_s = 2\pi/\omega_s = 6.25$ ns, as shown in Fig. 1. Since the time for one sequence is $4\pi/\omega_s$, the force is $\sim 2\hbar k/(4\pi/\omega_s) = \hbar k\omega_s/2\pi$. The direction of the frequency sweep, namely the sign of $\dot{\delta}$, is of no consequence as long as $\vec{\Omega}'$ is essentially polar at the ends of the sweep.

If spontaneous emission occurs during an excitation pulse, the returning pulse would excite the resulting ground state atoms, but the momentum transfer would be in the wrong direction, thereby reversing the force. Since such events are always possible, our pulse repetition rate is $\omega_s/4\pi$ to allow some time in the dark for such atoms to decay (see Fig. 1). Nevertheless, the force will be reversed for about 25% of the time and so the average force over very many lifetimes would be $F_{ARP} \sim \hbar k\omega_s/4\pi \gg F_{rad}$. For our modulation frequency $\omega_s = 2\pi \times 160$ MHz $\approx 100\gamma$, this picture predicts $F_{ARP} \sim 16\, F_{rad}$. This is very similar to the schemes proposed in Refs. [11,13].

Our apparatus for the study of polychromatic forces on metastable $2\,^3S_1$ He (He*) has already been described [3,5], but is briefly reviewed here. Our atomic beam source is modeled after the reverse flow design of Shimizu [19] with modifications originated by Mastwijk *et al.* [20], as described in Refs. [3,5]. The atoms have a distribution of longitudinal velocities v_ℓ and pass through a vertical 300 μm slit to define and collimate the beam in order to enable one-dimensional (1D) transverse measurements of atomic deflection.

We use a microchannel plate (MCP) and phosphor screen combination to detect the He* atoms $L = 50$ cm away from the interaction region, and we infer the transverse velocity imparted by ARP from their measured spatial distribution. Since He* atoms carry about 20 eV of internal energy, they can eject an electron from the upstream surface of the MCP with high probability, and the amplified electron signals at the output side of the MCP are accelerated to the screen. The screen is viewed through a window by a video camera connected to a PC via a frame grabber card.

We drive the $2\,^3S_1 \to 2\,^3P_2$ transition [$\tau(2\,^3P_2) \approx 97$ ns] at $\lambda = 1083$ nm using light from a diode-pumped fiber amplifier [21] that originates from an SDL-6702-H1 diode laser. The light is frequency modulated by a Photline model NIR-MPX-LNO3 [22], amplified by a Keopsys model OIYB30 fiber amplifier, amplitude modulated by a Photline model NIR-MX-LNO3, and amplified again by a Keopsys model KPS-BT2-YFA amplifier to produce the necessary 1 to 2 W of appropriately modulated light.

In developing instruments for these experiments, we have exploited recent developments in optical communications. The Photline modulators have proton-exchanged $LiNbO_3$ waveguides with V_π as low as 4.5 V and thus require relatively low rf power for the modulation. Synchronized driving of the two modulators produces the necessary multiple ARP sequences of 3 ns chirped pulses that span up to a few GHz, as needed for the experiment. The pulse profiles produced by the amplitude modulator are measured with a fast photodiode (see Fig. 2). Others have addressed similar topics [23].

By contrast, measurement of the frequency sweeps is not so simple. To begin, the atoms respond to the sweeps at a rate $|\Omega'| \gg \omega_s$ so they see the instantaneous optical frequency that is required for ARP. For sinusoidal frequency and phase modulation, the optical electric field for $0 < t < T_s$ is

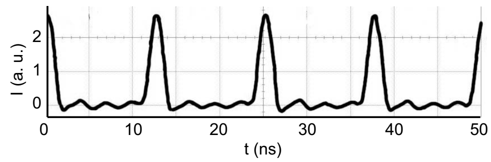

FIG. 2. The light pulses as measured by a fast photodiode. Their repetition rate is $\omega_s/4\pi=80$ MHz and their width at their base is $\sim\pi/\omega_s=3.125$ ns.

$$\vec{\mathcal{E}}(t)=\underbrace{\vec{\mathcal{E}}_0\sin(\omega_s t)}_{\text{amplitude}}\cos\underbrace{[\omega_\ell t+\beta\sin(\omega_s t)]}_{\text{phase}}, \tag{2}$$

where ω_ℓ is the laser frequency and $\beta\equiv\delta_0/\omega_s$. Then the instantaneous frequency is the time derivative of the phase of $\vec{\mathcal{E}}(t)$, namely $\omega_\ell+\delta_0\cos(\omega_s t)$ which provides just the desired frequency sweep of $2\delta_0$ in time π/ω_s.

However, a Fabry-Perot spectrum analyzer that can resolve ~40 MHz has a ring-down time of ~10 ns, comparable to $\pi/\omega_s\sim$ several ns, so it shows the familiar time averaged spectrum as a carrier with sidebands. For the case of pure phase modulation, our measured spectra show the textbook Bessel-function dependence of the frequency components. Typical measured spectra with amplitude modulation agree well with the calculated Fourier transform of Eq. (2), and are shown in Fig. 3.

The output beam of the second amplifier is subsequently circularly polarized to pump atoms into the $M_J=1$ sublevel of the $2\,^3S_1$ state and to drive the closed transition to the $2\,^3P_2$, $M_J=2$ sublevel. The peak Rabi frequency in our elliptical Gaussian laser beams (waists ~7 and 2.1 mm) is

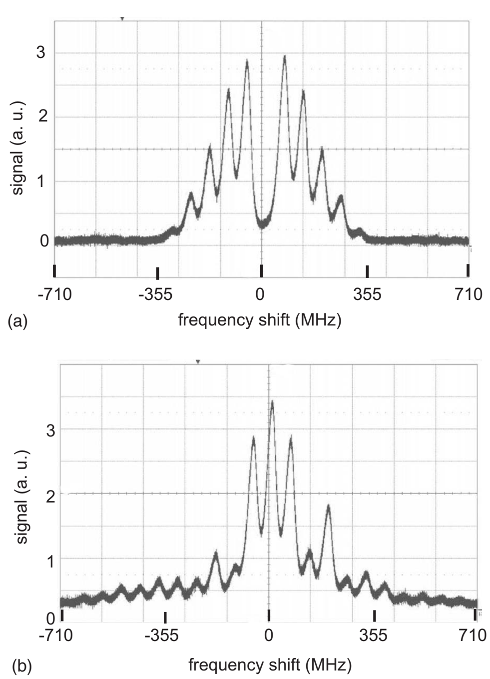

FIG. 3. Measured Fabry-Perot spectra. Part (a) shows the spectrum of the amplitude-modulated light as depicted in Fig. 2. Part (b) shows the spectrum of light delivered to the atoms as depicted in Fig. 1.

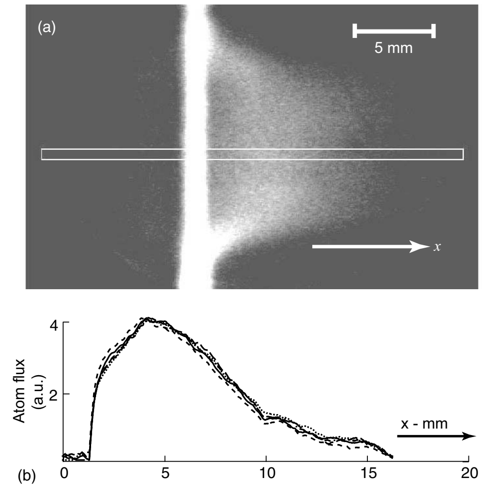

FIG. 4. Part (a) shows an image of the phosphor screen illuminated by electrons amplified by the MCP that are emitted by impact of He* atoms and uv light from the source discharge. The bright vertical line whose center is at $x=0$ is the image of the collimating slit produced by the uv, and the broad smear to its right results from the deflected atoms. The height of the smear in the region of strong deflection corresponds to the vertical variation of the Gaussian laser beam intensity of more than 40%. The interaction time was $\sim30\tau$ ($d\sim3$ mm), $\delta_0\approx5.57\omega_s$, and $\Omega_0\sim4.3\omega_s$. The four overlapping curves of part (b), made by averaging in the box indicated in part (a) after subtraction of the uv, are plots of the atomic flux from four separate images whose Ω_0 values ranged from 3.66 to 4.31 ($\times\omega_s$). This corresponds to an intensity range of ~30%, and together with the height of the smear in part (a), clearly shows the robustness of the ARP force against intensity variations. (The sharp cutoff and flat bottom toward the left end of these traces results from the subtraction of the slit image produced by the uv light from the source discharge.)

$\sim400\gamma\approx4\omega_s$ corresponding to ~53 W/cm^2, about $3.2\times10^5 I_{sat}$, where the saturation intensity $I_{sat}\equiv\pi hc/3\lambda^3\tau$ ≈0.167 mW/cm^2. In the horizontal direction, parallel to the atomic beam, the 14 mm wide laser beam is occluded at the edges by an adjustable vertical slit of width $d\sim3$ mm so the Rabi frequency seen by the atoms varies by only ~4.5% and also to limit the interaction time to ≈3 μs ($\sim30\tau$) since $v_\ell\sim1000$ m/s.

We viewed the atomic distribution at the end of the beam line with a video camera and saved the image; a typical one is shown in Fig. 4(a). The four overlapping curves of Fig. 4(b) are the atomic flux values taken by averaging over a box as shown in Fig. 4(a) after subtraction of a background of uv light from the source discharge.

Our analysis begins with the assumption that the ARP force is constant during the atoms' flight through the laser beams. Because x, the transverse displacement at the detector of atoms that gain equal transverse velocities from ARP, is $\propto1/v_\ell^2$ we find $\langle1/v_\ell^2\rangle$ from the previously measured longitudinal velocity distribution [3]. We also find $\langle x\rangle$ from data similar to those of Fig. 4(b) and then calculate the force $F_{\text{meas}}=[\langle x\rangle/Ld]\times[M/\langle1/v_\ell^2\rangle]$, where M is the atomic mass. (The asymmetry of the distributions requires this care with the averages.)

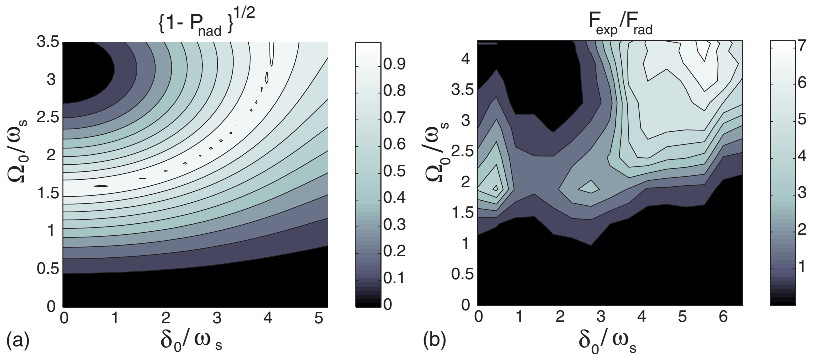

FIG. 5. (Color online) Part (a) shows a calculated map of the force from the nonadiabatic transition probabilities in Ref. [1], and part (b) shows the force we extracted from our measurements by the analysis described above. Lighter areas correspond to larger forces. The qualitative agreement is quite excellent. These strong forces appear where Ω_0 and δ_0 are $\sim(4-5)\times\omega_s$, values that do not satisfy the $\gg$ criterion of Eq. (1) very well.

The average x value of the distributions in Fig. 4(b) is $\sim$5.6 mm corresponding to a transverse velocity of $\sim$11 m/s$\sim$120$\times$ the recoil velocity $\hbar k/M \approx 9.2$ cm/s. The resulting $F_{meas} \sim 7F_{rad}$, more than 40% of the estimated $\hbar k \omega_s/4\pi \sim 16F_{rad}$.

The key to a large force using ARP is prevention of nonadiabatic transitions whose probability P_{nad} has been calculated in Ref. [1]. More recently we have shown that the force is $\propto\sqrt{1-P_{nad}}$ [18], and in Fig. 5(a) we have plotted this expected force versus the parameters δ_0 and Ω_0. In Fig. 5(b) we plot F_{meas} over this same range of parameters for comparison. The qualitative agreement is clear. These strong forces appear where Ω_0 and δ_0 are $\sim(4-5)\times\omega_s$, values that do not satisfy the $\gg$ criterion of Eq. (1) very well but are predicted by the model of Fig. 5(a). Needless to say, the region of parameter space just above the right-hand side of these plots is crying for exploration but we presently have technical limitations.

We attribute the majority of the discrepancy between F_{meas} and F_{ARP} to two sources. First, He* has $J=1$ and atoms entering the interaction region with $M_J=-1$ experience a $\sqrt{6}$ times lower Rabi frequency in the σ^+ light than those with $M_J=+1$ (Clebsch-Gordan coefficient). A simple model suggests that optically pumping them to $M_J=+1$ (into the cycling transition) takes a significant fraction of the interaction time so they experience less force. Those entering with $M_J=0$ are also subject to somewhat less force, and the net expectation is a broader distribution with significantly less average deflection. Second, our model of ARP is only a model: it does not fully account for the effects of spontaneous emission (including diffusion in momentum space [13]) and for the coherence effects. A full density matrix treatment of this problem could easily produce a weaker force. Along with our nonideal pulse shapes, we estimate that these effects combine to account for most of the discrepancy.

We mapped the ARP force produced by counterpropagating chirped light pulses over a region of parameter space of $(\delta_0/\omega_s, \Omega_0/\omega_s)$ and found qualitative agreement with our model. The force is very robust against the variations of these parameters. Its magnitude and velocity range are much larger than those of the usual radiative force, but may be compromised by the atomic distribution among the M_J states. A planned optical pumping stage should eliminate this difficulty. We believe that the fully implemented ARP force could stop our He* beam in a distance of less than 1 cm, much shorter than the 2 m required to stop He* with F_{rad} [2].

This research was supported by the Office of Naval Research and the Army Research Office.

[1] T. Lu, X. Miao, and H. Metcalf, Phys. Rev. A **71**, 061405(R) (2005).

[2] H. Metcalf and P. van der Straten, *Laser Cooling and Trapping* (Springer, New York, 1999).

[3] M. Cashen and H. Metcalf, Phys. Rev. A **63**, 025406 (2001).

[4] M. Cashen, O. Rivoire, V. Romanenko, L. Yatsenko, and H. Metcalf, Phys. Rev. A **64**, 063411 (2001).

[5] M. Cashen, O. Rivoire, L. Yatsenko, and H. Metcalf, J. Opt. B: Quantum Semiclassical Opt. **4**, 75 (2002).

[6] L. Yatsenko and H. Metcalf, Phys. Rev. A **70**, 063402 (2004).

[7] M. Partlow, X. Miao, J. Bochmann, M. Cashen, and H. Metcalf, Phys. Rev. Lett. **93**, 213004 (2004).

[8] V. Voitsekhovich, M. Danileiko, A. Negriiko, V. Romanenko, and L. Yatsenko, Zh. Tekh. Fiz. **58**, 1174 (1988) [Sov. Phys. Tech. Phys. **33**, 690 (1988)].

[9] V. Voitsekhovich, M. Danileiko, A. Negriiko, V. Romanenko, and L. Yatsenko, Pis'ma Zh. Eksp. Teor. Fiz. **49**, 138 (1989) [JETP Lett. **49**, 161 (1989)].

[10] J. Söding, R. Grimm, Y. Ovchinnikov, P. Bouyer, and C. Salomon, Phys. Rev. Lett. **78**, 1420 (1997).

[11] I. Nebenzahl and A. Szoke, Appl. Phys. Lett. **25**, 327 (1974).

[12] V. Voitsekovich, M. Danileiko, A. Negriiko, V. Romanenko, and L. Yatsenko, Ukr. Fiz. Zh. **36**, 192 (1991).

[13] G. Demeter, G. Djotyan, and J. Bakos, J. Opt. Soc. Am. B **15**, 16 (1998).

[14] M. Cashen and H. Metcalf, J. Opt. Soc. Am. B **20**, 915 (2003).

[15] R. Feynman, F. Vernon, and R. Hellwarth, J. Appl. Phys. **28**, 49 (1957).

[16] L. Allen and J. Eberly, *Optical Resonance and Two-Level Atoms* (Dover, New York, 1987).

[17] D. Sawicki and J. H. Eberly, Opt. Express **4**, 217 (1999).

[18] X. Miao, Ph.D. thesis, Stony Brook University, 2006 (unpublished).

[19] J. Kawanaka, M. Hagiuda, K. Shimizu, F. Shimizu, and H. Takuma, Appl. Phys. B: Photophys. Laser Chem. **56**, 21 (1993).

[20] H. C. Mastwijk, Ph.D. thesis, University of Utrecht, Netherlands, 1997 (unpublished).

[21] Keopsys Corp., Lannion, France.

[22] Photline Corp., Besançon, France.

[23] C. Rogers, III, M. Wright, J. Pechkis, J. Carini, and P. Gould, J. Opt. Soc. Am. B (to be published).